

HCN Channels as Targets for Drug Discovery

Michael P. Maher, Nyan-Tsz Wu, Hong-Qing Guo, Adrienne E. Dubin, Sandra R. Chaplan and Alan D. Wickenden*

Johnson & Johnson Pharmaceutical Research and Development, L.L.C., San Diego, CA 92121, USA

Abstract: Hyperpolarization- and Cyclic Nucleotide-gated (HCN) channels are a family of six transmembrane domain, single pore-loop, hyperpolarization activated, non-selective cation channels. The HCN family consists of four members (HCN1-4). HCN channels represent the molecular correlates of I_h (also known as 'funny' I_f and 'queer' I_q), a hyperpolarization-activated current best known for its role in controlling heart rate and in the regulation of neuronal resting membrane potential and excitability. A significant body of molecular and pharmacological evidence is now emerging to support a role for these channels in the function of sensory neurons and pain sensation, particularly pain associated with nerve or tissue injury. As such, HCN channels may represent valid targets for novel analgesic agents. This evidence will be reviewed in this article. We will then summarize our efforts to develop and validate methods for screening for novel HCN channel blockers.

INTRODUCTION

Nociception, or the sensation of pain, is a function vital to the survival of higher organisms. The normal physiological function is to signal the brain that potential or actual damage has occurred. Under pathological conditions, nociceptive nerve fibers can become hyperexcitable or even spontaneously active. Nerve injury often induces rhythmic or bursting behavior in afferent fibers [1, 2]. This curious phenomenon led some investigators to consider the role of 'pacemaker' channels in these neurons.

Pacemaking currents were first functionally described as the 'funny' current I_f in rabbit sinoatrial node [3] and the 'queer' current I_q in hippocampal pyramidal neurons [4]. These excitatory currents push a cell towards the threshold of activation for action potentials. In cardiac tissue, adrenergic stimulation increases intracellular cAMP, upregulating I_f , which leads to a higher heart rate.

The molecular basis for the pacemaker currents was identified when a novel family of ion channels with homology to cyclic-nucleotide gated channels were cloned [5-7]. HCN channels are a family of six transmembrane domain, single pore-loop, hyperpolarization activated, non-selective cation channels. The HCN family consists of four members (HCN1-4). HCN channels represent the molecular correlates of I_f and I_q (now referred to collectively as I_h). A significant body of molecular and pharmacological evidence is now emerging to support a role for these channels in the function of sensory neurons and pain sensation, particularly pain associated with nerve or tissue injury [8]. As such, HCN channels may represent valid targets for novel analgesic agents. This evidence will be briefly reviewed in the following article. We will then summarize our efforts to develop and validate methods for screening for novel HCN channel blockers that may be useful for the treatment of chronic pain.

EXPRESSION AND FUNCTION OF HCN CHANNELS IN SENSORY NERVES

The presence of I_h has been demonstrated in a variety of peripheral sensory nerve preparations, such as rat DRG [9-18], mouse DRG [19-21], rat and rabbit nodose ganglia [22, 23] and guinea-pig myenteric neurons [24]. A consistent finding in these studies, regardless of the species or preparation, is that I_h appears more prominent in large diameter A β neurons, compared to small or medium diameter cells [9, 10, 14, 17, 18, 20, 22, 23, 25].

Under resting conditions, I_h blockers, such as ZD-7288, clonidine and zatebradine (UL-FS49), have little or no effect on sensory nerves [10, 15, 18, 21, 26]. In keeping with a rather limited role in healthy sensory neurons, the use of I_h blocking drugs is typically not associated with sensory side-effects such as dysesthesia and paresthesia [27]. In contrast, several recent publications suggest that I_h may be required to support spontaneous sensory nerve activity and the development and/or maintenance of allodynia that occurs as a result of nerve and tissue injury. For example, ZD-7288 has been shown to inhibit injury induced ectopic neuronal discharges in isolated spinal nerves and in damaged nerves *in situ* [16, 28, 29]. The same compound also exhibits anti-allodynic effects in the spinal nerve ligation model (Chung model) and in a model of partial sciatic nerve ligation [Seltzer model; 16, 28, 30]. More recently, ZD-7288 has been shown to inhibit spontaneous pain and tactile allodynia resulting from acute insults such as a mild thermal burn and skin incision [30, 31]. Just how block of I_h can inhibit injury-induced spontaneous pain and allodynia is not fully understood. However, injured nerves are known to fire action potentials at high frequencies (typically 10 – 100 Hz), and I_h may be required to prevent conduction failure at these high frequencies [32]. Inhibition of spontaneous firing and allodynia following nerve injury may therefore, be a function of the ability of I_h blockers to preferentially suppress high frequency firing. Alternatively, the function of I_h may become dominant in the setting of tissue/nerve injury leading to the emergence of I_h -driven pacemaker-like (ectopic) activity. An

*Address correspondence to this author at the Johnson & Johnson Pharmaceutical Research & Development, L.L.C., 3210 Merryfield Row, San Diego, CA 92121; Tel: (858) 320-3447; Fax: (858) 450-2040; E-mail: awickend@prdus.jnj.com

increase in the functional importance of I_h may result from changes in HCN expression relative to other ion channels [13-16, 33-36]. Alternatively, the function of I_h may become dominant in the setting of tissue/nerve injury as a result of local modulation by inflammatory mediators such as PGE₂, 5-HT, and substance P [11, 37, 38].

THE MOLECULAR BASIS OF I_h IN SENSORY NERVES

Molecular studies have examined the expression of HCN1 - 4 in peripheral sensory neurons. Using in-situ hybridization, Moosmang *et al.* found that the predominant HCN sub-unit in mouse DRG cells was HCN1, followed by HCN2, with the highest expression levels in large diameter neurons [39]. HCN3 and HCN4 mRNA was undetectable. Several groups have now confirmed and extended these initial observations, at both the mRNA and protein level in various sensory nerve preparations [16, 17, 40]. In skin, Luo and colleagues have demonstrated HCN1, HCN2 and HCN3-like immunoreactivity in specialized mechanosensitive nerve endings such as Meissner's corpuscles and Merkel cells [31]. HCN1 and HCN2 have also been detected on the central terminals of sensory nerves in the spinal dorsal horn [17, 41-44].

As a complimentary approach to the identification of the key isoforms responsible for I_h in sensory neurons, several groups have attempted to correlate the properties of I_h in sensory nerves with those of heterologously expressed recombinant HCN channels. The properties of HCN channels have been reviewed in detail recently by Robinson and Siegelbaum [45] and will not be covered in detail in the present article. However, it is worth noting that the various HCN channel sub-types differ significantly in their activation kinetics, with HCN1 exhibiting fastest activation, and HCN4 the slowest activation [39, 46, 47]. The properties of HCN2, HCN3 and heteromeric HCN complexes tend to exhibit intermediate properties [48]. Activation rates of I_h in large and medium diameter sensory neurons are fast and comparable to activation rates measured for HCN1 and/or HCN2. The available data on I_h activation rates in small diameter sensory neurons is somewhat variable, possibly as a result of the small current amplitude in these cells and associated difficulties in obtaining accurate fits. However, on average, activation appears slower in small compared to medium and large cells [17, 18, 23].

HCN sub-types also differ in their sensitivity to cAMP. Cyclic AMP increases HCN based currents by shifting the voltage-dependence of activation in a depolarizing direction (i.e. greater open probability at physiological potentials). In a side-by-side comparison, Steiber *et al.* reported shifts of 6.2 mV, 28.5 mV, -2.9 mV and 23 mV for human HCN1, HCN2, HCN3 and HCN4, respectively, on addition of 100 μ M 8-Br-cAMP [47]. Most published studies indicate that cAMP has only modest effects on I_h in sensory neurons, with shifts between 0 - 10.7 mV depending on the sensory nerve preparation [11, 37, 40, 49].

In summary, I_h is a prominent current in many peripheral sensory nerves, with highest current density typically found in large diameter neurons. Recent data suggests that I_h may be necessary to support the high frequency firing typically found in injured sensory nerves. As such, I_h may represent a

valid target for the treatment of spontaneous pain and allodynia associated with nerve injury. The majority of available electrophysiological and molecular evidence suggests that fast activating, weakly cAMP sensitive HCN1-based channels may make a significant contribution to I_h especially in large diameter fibers. Therefore, we set out to identify HCN1-selective pharmacological tools. In the remainder of this article we describe the development and validation of assays suitable for high throughput screening of novel HCN blockers.

ASSAY PRINCIPLE

HCN channels are permeable to both sodium and potassium, with a permeability ratio $P_{Na}/P_K \sim 0.25$ and reversal potential near -25 mV in physiological saline [7, 32]. They are relatively impermeant to divalent cations, and show no measurable inactivation. Under physiological conditions, open HCN channels pass inward sodium and outward potassium currents. However, if we replace extracellular sodium with an impermeant cation, both sodium and potassium feel a net outward driving force. The reversal potential of the channel, as determined by the Goldman-Hodgkin-Katz (GHK) equation, approaches that of potassium alone.

HEK cells have resting potentials at approximately -50 mV due to their endogenous potassium channels [50]. Heterologously-expressed HCN channels have activation voltages in the range -80 to -90 mV, so a small (but non-zero) fraction of channels is open. In the presence of extracellular sodium, the resulting HCN current is too small to affect the resting potential due to the endogenous potassium currents. In the absence of extracellular sodium, these open channels exert a hyperpolarizing influence on the cell, opening yet more HCN channels, so that the resting potential is driven towards $E_K \sim -100$ mV. If the HCN channels are inhibited, the membrane potential will still be maintained near -50 mV by the endogenous currents. This difference in resting potential provides the basis for the assay. If extracellular sodium is re-introduced, it will flow through open HCN channels, depolarizing the cell towards the normal HEK resting potential. If the channels are inhibited, no change in membrane potential will occur.

To discover novel pharmacological agents as inhibitors of HCN channels, we developed a functional assay with the intent to screen a large, diverse library of compounds. Several techniques are available for testing the pharmacology of ion channel targets, including electrophysiology, competitive binding, and optical sensors. Although electrophysiology is inherently the most accurate method, the throughput (tens to hundreds of compounds per day) is far too low for modern screening campaigns [51]. While meeting throughput requirements, binding assays probe a single binding site and may not detect novel modulators. They also require a fluorescently or radioactively labeled high-affinity probe molecule, which has not yet been discovered for HCN channels.

Optical assays are well-suited for massively-parallel high throughput screening campaigns. Activity of HCN channels is most conveniently measured using dyes sensitive to the cell membrane potential. We chose to use a FRET-based voltage-sensitive dye system in a Voltage-Ion Probe Reader (VIPR™, Aurora Biosciences Corp.) [52]. This platform tends to give faster responses than other Nernstian redistribu-

tion dyes (~1 s vs 1-5 min), and the ratiometric nature of the response tends to reduce sensitivity to artifacts. Detailed methods are described in Appendix 1.

PROOF OF PRINCIPLE

We first checked the basic performance of the assay by comparing the responses of HEK cells stably expressing human HCN1 with untransfected HEK cells in the presence and absence of an HCN channel antagonist (5 mM cesium). Fig. (1) shows the time course of the normalized fluorescence ratio. The cells started the assays in zero-sodium buffer, then the sodium concentration in the well was brought to 65 mM at $t = 12$ sec. Untransfected cells had virtually no response, indicating that this drastic change in buffer had minimal effects on the membrane potential dyes and on endogenous processes in the cell. HEK-HCN1 cells responded with a rapid increase in fluorescence ratio, followed by a slow decline, consistent with a net depolarizing change in membrane potential. In the presence of a blocking concentration of cesium, the fluorescence ratio had a much smaller increase that subsequently declined below the starting value. Interestingly, the transient response in the cesium-blocked HEK-HCN1 cell response was noticeably larger than for the untransfected cells. We did not further investigate this phenomenon.

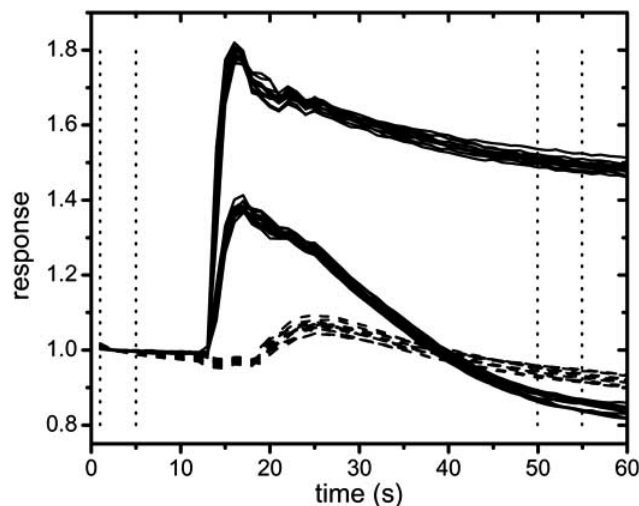


Fig. (1). Time course of the response of HEK-HCN1 cells in the sodium add-back assay. The two populations of solid lines are twelve individual wells each of negative (no antagonists; upper set of curves) and positive (5 mM cesium; lower set of curves) control wells. The responses of untransfected HEK cells under the same assay conditions are also shown (dashed lines). The dotted vertical lines indicate the measurement windows used for subsequent calculations.

To further demonstrate that these responses were mediated by HCN, we determined the ability of known antagonists to block the response in the VIPR assay. Fig. (2A) shows the response as a function of concentration of zatebradine, ivabradine, alinidine, and ZD-7288. In these assays, responses were normalized to negative (no added compounds) and positive (5 mM cesium chloride) controls. At sufficiently high concentration, each compound fully blocked the response. Generally, most compounds have very

steep dose-response curves with Hill slopes substantially larger than one (see Discussion).

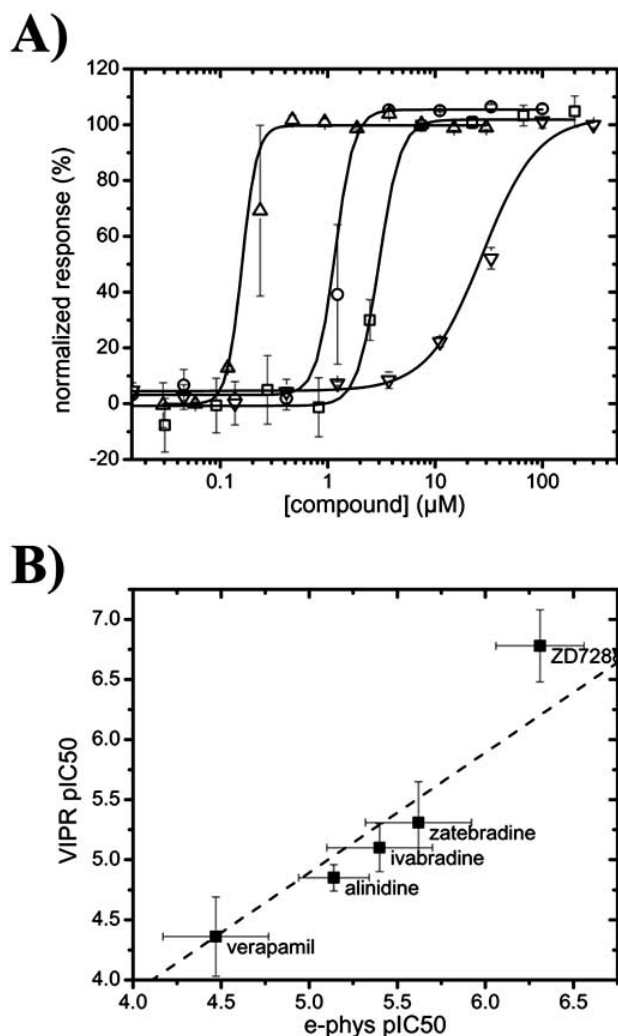


Fig. (2). Pharmacology of known HCN antagonists. (A) Representative concentration-response curves for zatebradine (\square), ivabradine (\circ), ZD-7288 (Δ), and verapamil (∇) as measured using the VIPR sodium add-back assay. (B) Comparison of pIC_{50} values measured at -100 mV using electrophysiology on HEK-HCN1 cells to pIC_{50} from the VIPR assay. Data points are the average and standard deviations of $N=3-8$ cells for electrophysiology, and 4-80 full dose-responses for the VIPR assay. The dashed line is a linear fit to the data.

We also measured the potency of the compounds to block the HCN current using whole-cell patch clamp electrophysiology. Many HCN antagonists demonstrate use- and/or voltage-dependent behavior, so to match the VIPR assay as closely as possible, we determined the steady-state block at -100 mV. Fig. (2B) compares the potency of several antagonists as measured using VIPR and electrophysiology. The dashed line is a linear fit to the data with the slope fixed at one; the correlation for this fit is $r=0.95$.

Assay Optimization

With a firm theoretical basis for the assay, a substantial dynamic range, and the proper pharmacology, we proceeded

to optimize the assay. In a large screening campaign, it is critical to know how tightly each aspect of the process must be controlled. The goal of this process was to maximize the stability of the response with respect to all of the variables that have an effect. This includes dye concentrations, ion concentrations in the starting and final buffers, cell density, culture time, time in low-sodium buffer, etc. Stability is assessed by the screening window z' [53] and the measured potency of standard compounds. With so many interdependent variables, it would be impossible to test every combination. Therefore, we checked each parameter separately and searched for regions with minimal variance. This exercise also served to find the limits of tolerance and mode of failure for each parameter.

Dye Concentration

We stained cells in a 96-well plate with orthogonal gradients of each dye, and then performed the sodium add-back assay. The plate was seeded at 50K cells/well 24 h prior to the assay, at which time the cells were nearly confluent. Fig. (3A) shows a contour plot of the response as both dye concentrations were varied. A large plateau with responses in the range 1.4-1.5 covered most of the space, suggesting that the assay was very stable to even large changes in dye concentrations.

Another factor to consider is the brightness of the signal; higher fluorescence intensity protects against contamination by dust, variations in background fluorescence, fluorescent test compounds, etc. Fig. (3B) and (3C) show contour plots of the donor (blue) and acceptor (red) signals normalized to the background fluorescences of an empty plate. As expected, the blue signal (Fig. 3B) increased monotonically as the CC2-DMPE concentration increased. This trend reversed above 16 μM CC2-DMPE, possibly due to the solubility of this dye. Consistent with FRET, the blue signal decreased substantially as the acceptor concentration increased. The red signal, shown in Fig. (3C), was proportional to the concentration of both dyes, again consistent with substantial FRET from the donor.

Based upon this set of data, and the desire to limit costs by minimizing reagent use, we chose to proceed with 3 μM DiSBAC₂(3) and 6 μM CC2-DMPE for the assay. This was well within the plateau region for the magnitude of the response, and gave signal/background values near 2 for both donor and acceptor.

Cell Density

Some cell-based assays are dependent upon cell density or the degree of confluence at the time of the assay. We tested for such an effect by seeding different densities of cells into entire columns 96- and 384-well plates, and cultured them for 24 h prior to the assay. At the time of the assay, the cells were nearly confluent when plated at 50K/well in the 96-well plate and 25K/well in the 384-well plate. We used 5 mM cesium chloride in half of the wells as a positive control.

Fig. (4) summarizes the responses of these cells in the sodium add-back assay. The control responses were relatively uniform above 30K/well for the 96-well plate, and above 15K/well for the 384-well plate. Above these densities, the screening windows z' averaged 0.85 for the 384-

well plate and 0.66 for the 96-well plate. We also observed that the fluorescence intensity reached plateaus at confluence. Thus, for the assay, we chose to use 50K/well for 96-well plates, and 25K/well for 384-well plates.

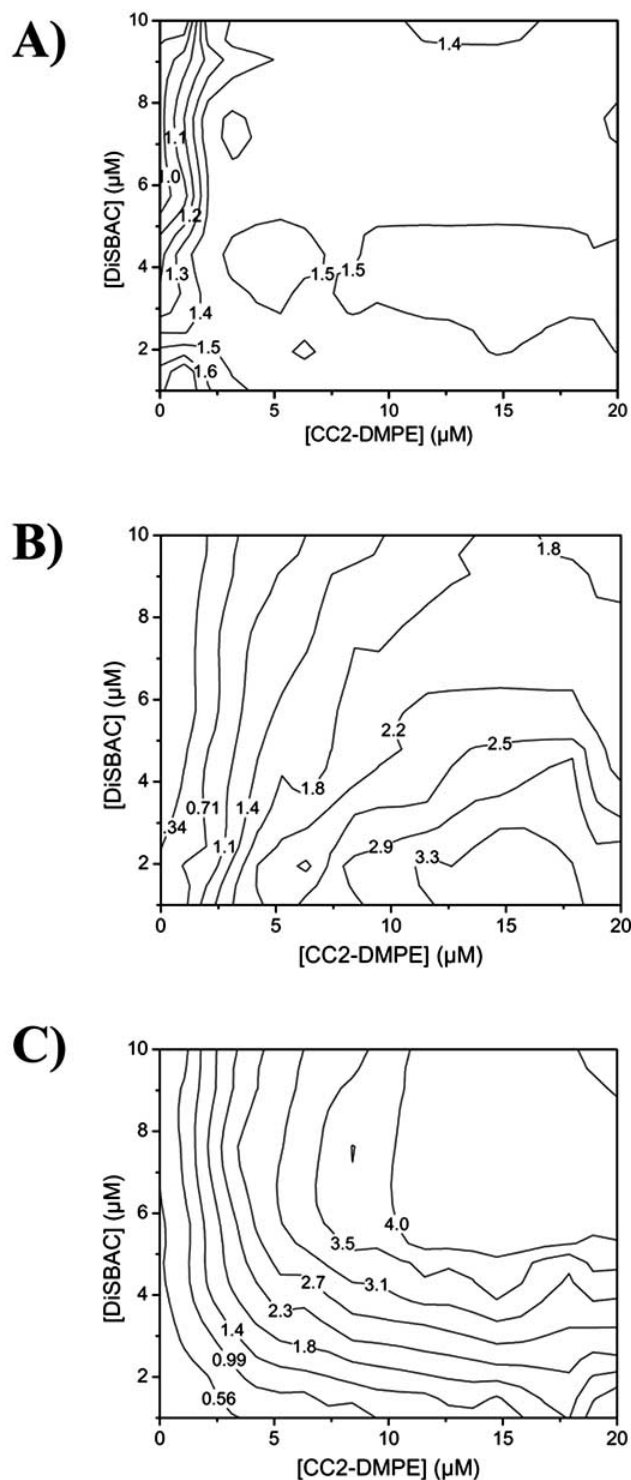


Fig. (3). Dye optimization for the sodium-addback assay for HEK-HCN1. Data are represented as contour plots. (A) Normalized fluorescence ratio change. (B) Blue (440 nm) signal/background. (C) Red (580 nm) signal/background.

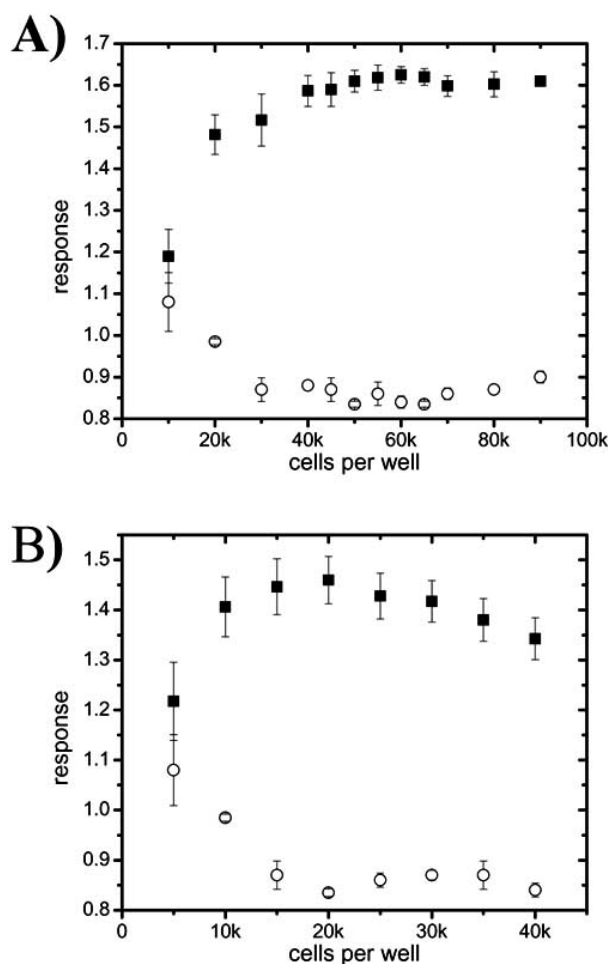


Fig. (4). Optimization of the assay for cell density. The response for negative (■) and positive (○) control wells as functions of the cell density, plated 24 h prior to the experiment. Data are the mean and standard deviation for all wells on the plates (half with 5 mM Cs⁺, half without). (A) 96-well plate. (B) 384-well plate.

Time in Culture

Numerous processes occur after seeding the cells that have the potential to affect the assay, including attachment, cell growth, protein synthesis and degradation, exhaustion of nutrients in the medium, etc. To explore this issue, we measured the response at multiple time points between seeding cells into 384-well plates and performing the sodium add-back assay. No test compounds or positive controls were used in this experiment. We noted that when initially seeded, cells were roughly 50% confluent, reaching confluence at around 24 h. The cell doubling time under normal conditions was approximately 1 day.

Fig. (5) shows the average and standard deviation of all wells in the plate at each time point. In all measurements, the standard deviation is relatively small. The response has a small increase between 14 and 24 h post-seeding, possibly reflecting the sub-confluent density during this period (Fig. 4B). The response remained at approximately 1.5 for 24–54 h, and then slowly declined. After 48 h, the culture medium was acidic and the cells were overgrown. Thus, the assay had a very stable response in the range of 24–48 h after seeding

the cells. This would potentially simplify the scheduling and cell culture requirements during an extended screening campaign.

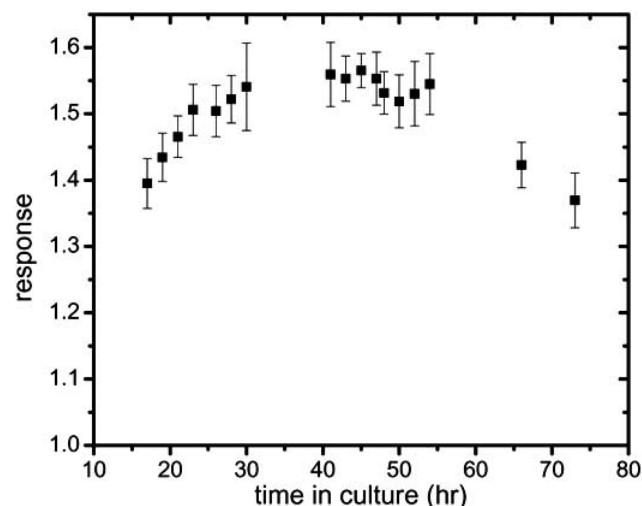


Fig. (5). Response of HEK-HCN1 cells to the sodium addback assay as a function of time in culture. Cells were plated into 384-wells plates at 25K cells/well. Data are the mean and standard deviation of all 384 wells on each plate.

Tolerance to Sodium

The assay requires the cells to start in a low extracellular sodium buffer, to hyperpolarize the resting potential of the cell. Although the rinse steps in the assay should reduce the extracellular sodium to below 0.1 mM, the reagents used in the assay did not have strict quality control for the presence of sodium. To explore this issue, we measured the response as functions of the initial and final sodium concentrations by mixing the sodium-free and sodium buffers.

To vary the initial sodium concentration, we added varying amounts of sodium to the cell plates before running the assay. In this experiment, the sodium add-back was still a 2:1 dilution of the 130 mM NaCl buffer, so the final sodium concentration varied slightly (from 65 to 67 mM). Fig. (6A) summarizes the results. There is a surprisingly small dependence of the response to modest changes in the sodium concentration, with a slight trend towards a smaller response at higher starting sodium concentration.

When we altered the sodium concentration in the add-back buffer, there was a more pronounced trend towards smaller responses with lower sodium concentration (Fig. 6B). Still, there was very little sensitivity to sodium concentration in the upper end of the range (50–65 mM NaCl). In this experiment, the cells began the assay in nominally zero extracellular sodium.

To understand this phenomenon, we estimated the HCN reversal potential as a function of sodium concentration using the GHK [55] equation. We assumed that the maximal response corresponded to the maximal membrane potential change predicted by the GHK equation, and that the negative control response corresponded to no change in membrane potential. The correspondence between the assay response and the on the membrane potential on the right axis was not directly calibrated, and is shown only to illustrate the ex-

pected trends. The curves in Fig. (6) are the resulting predictions for the membrane potential changes under these assay conditions, and they confirm the weak dependence of the response on the sodium concentration. Thus, the assay is relatively insensitive to sodium contamination in the initial buffer, and to variability in the final sodium concentration.

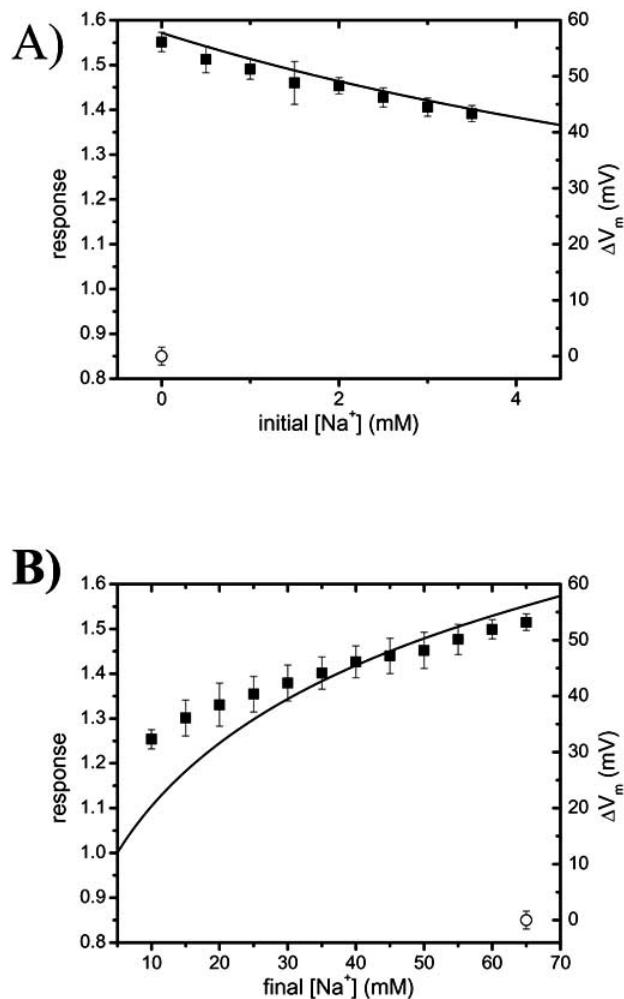


Fig. (6). Dependence of the response upon sodium concentration. Data points are the mean and standard deviation for the dye response for the negative (■) and positive (○) control wells (left axis). Solid lines are calculated from the Goldman-Hodgkin-Katz equation (right axis). (A) Variable sodium in the starting solution. (B) Variable sodium seen by the cells after the addback.

Time in Sodium-Free

Low extracellular sodium presumably has many deleterious effects, such as shutting down or reversing membrane transporters. To determine how long the cells can withstand low extracellular sodium, we varied the incubation times before running the assay. Fig. (7) shows the results of one such experiment. While the negative control response is very stable for 5 h, the response of the positive control (5 mM Cs^+) begins to increase after 2.5 h. At 5 h, the positive control response is nearly indistinguishable from the negative control, showing a substantial depolarization. This indicated that we needed to carefully monitor the timing for plate

processing, so that cell plates were used within 2.5 h of the first wash with zero-sodium buffer.

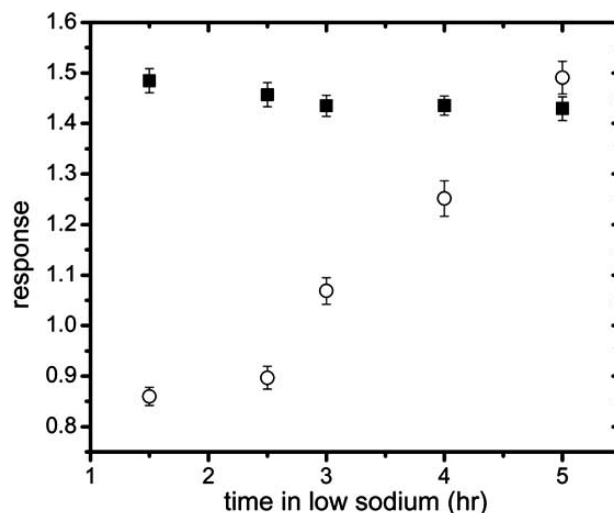


Fig. (7). Incubation in low sodium gradually erodes the difference between negative (■) and positive (○) controls.

DMSO Tolerance

DMSO is commonly used as a solvent for test compounds, and has been known to generate artifacts in cellular assays. The dose-response curve in Fig. (8) indicates that the assay is very tolerant to DMSO all the way up to 3%. These DMSO concentrations exceed those typically used in high throughput screening assays (generally 0.5-1%).

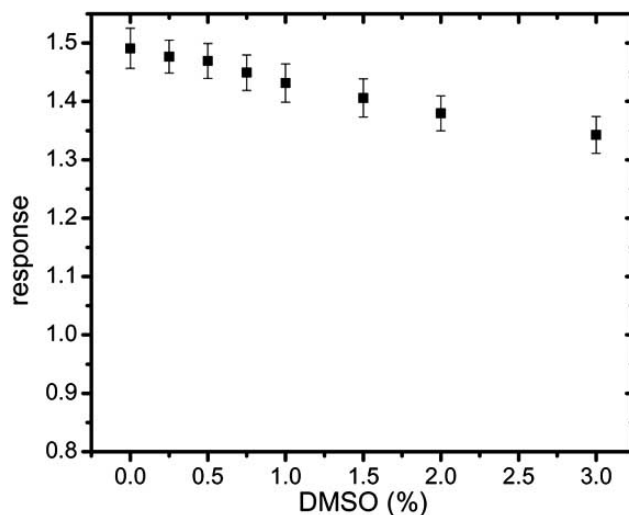


Fig. (8). Response in the presence of DMSO. Data points are the mean and standard deviations of 12 replicate wells.

SUMMARY

The non-selective cation channel HCN1 is a novel molecular target for the relief of pain, and has a relatively unexplored pharmacology. Here, we presented a summary of the development of a high throughput-compatible functional assay designed to detect antagonists of HCN1. This assay exploited the biophysical properties of the channel to set the membrane potential of stably transfected cells. Changing the ionic conditions during the assay caused changes in mem-

brane potential mediated by the activity of the channel, detected using voltage-sensitive fluorescent dyes.

In the absence of extracellular sodium, intracellular potassium exits the cell through open HCN channels and hyperpolarizes the membrane. If HCN is absent or pharmacologically blocked, hyperpolarization does not occur. While monitoring the membrane potential, we added sodium-containing saline. Cells with active HCN depolarize; only transient artifacts were seen when the channels were blocked. Conceivably, this assay principle could be used in several similar formats. Although we used a VIPR and ratiometric membrane potential dyes, several other voltage dyes and plate readers could be used instead. In fact, because the membrane potentials are sustained rather than transient, pre- and post- addback reads should suffice. Lastly, rather than adding sodium during the assay, one could determine the membrane potential in a zero-sodium saline before and after adding the test compound. Simply blocking the channel would cause the cell to depolarize.

The assay accurately reproduced the known pharmacology of the channel, as compared to measurements made using whole-cell electrophysiology. Several of the compounds tested, including ZD-7288, zatebradine, and alinidine, have complex state- and voltage-dependent activities. The electrophysiology data shown in Fig. (2B) was performed at steady-state at a holding potential of -100 mV to most closely match the expected conditions in the optical assay. However, the membrane potential is not clamped in the VIPR assay, and the actual potency of such compounds may be complex. The lack of voltage control in the VIPR assay may contribute to the steep dose-response curves we often see (Fig. 2A).

The assay presented here is a valuable new tool in the exploration of the pharmacology of the HCN channel family. The novel antagonists discovered may provide tools to further elucidate the biological functioning of the various HCN subtypes, and may form the basis for an entirely new class of analgesics.

MATERIALS AND METHODS

Reagents. DiSBAC₂(3), CC2-DMPE, and VABSC-1 were obtained from Invitrogen. Cell culture reagents were from Gibco. Pluronic F-127, assay buffer ingredients, and gramicidin were from Sigma.

The assay buffers were as follows (quantities in mM). Sodium-free buffer: 130 *N*-methyl-D-glucamine (NMDG), 2 KCl, 1 MgCl₂, 2 CaCl₂, 10 HEPES, 5 dextrose. Sodium buffer: 130 NaCl, 2 KCl, 2 CaCl₂, 1 MgCl₂, 10 HEPES, 5 dextrose. High-potassium buffer: 134 KCl, 2 CaCl₂, 1 MgCl₂, 10 HEPES, 5 dextrose. The buffers were adjusted to 300 mOs with water or the predominant salt, and pH 7.4 using HCl or the hydroxide of the predominant cation.

Dye stock solutions were 10 mM in dry dimethyl sulfoxide (DMSO). CC2-DMPE was diluted to 2X final concentration by adding the appropriate volume of stock solution plus an equal volume of 10% Pluronic F127 in DMSO into a plastic 50 mL centrifuge tube. Sodium-free buffer was added to the dye while vortexing. DiSBAC₂(3) was diluted to 2X final concentration by adding the appropriate volume of stock solution into a plastic 50 mL centrifuge tube. Sodium-

free buffer was added to the dye while vortexing, and then VABSC-1 was added to reach a concentration of 2 mM. The final concentrations seen by cells were 6 μ M CC2-DMPE and 3 μ M DiSBAC₂(3) unless otherwise noted.

Plasmid constructs and cell lines. Human HCN1 cDNA (accession number AF064876) was generated by PCR amplification from human spinal cord cDNA, and cloned into the pCDNA3.1 Zeo expression vector (Invitrogen) [16]. HEK-293 cells were transfected with this plasmid *via* lipofection, and a single-cell zeocin-resistant clone marker was isolated. Full-length transcription of HCN1 was verified by rtPCR, and functional expression was verified by whole-cell electrophysiology.

Cell culture. The cell lines were maintained in DMEM supplemented with 10% fetal bovine serum and the appropriate selection antibiotic in tissue culture flasks at 37°C in a 5% CO₂-95% air humidified atmosphere. Freshly dissociated HEK-293 cells were plated at 25,000 cells/well in 50 μ L/well of growth medium in 384-well poly-lysine coated plates (Becton-Dickinson BioCoat). For some experiments, 96-well plates were used (50,000 cells in 100 μ L/well). No differences were seen in the results obtained from the two different types of plate.

Optical assays. Growth medium was replaced with sodium-free buffer using a Biotek ELx405 plate washer. The washer performed 3 cycles, aspirating the well to 25 μ L then adding 75 μ L of buffer for 384-well plates. A final aspiration left 25 μ L of the new buffer. This process reduced the starting buffer by a factor of 64. The 2X CC2-DMPE solution was then added using a MultiDrop, then the cells were incubated for 30 min at room temperature in the dark. A second wash with sodium-free buffer removed the coumarin. Next, test compounds were added at 2X final concentration from 100X stock solutions in DMSO to a 96-well intermediate plate containing 2X DiSBAC₂(3) solution. The DiSBAC₂(3)/VABSC-1/test compound solutions were added to the cell plate following a second rinse with the plate washer. The cells were then incubated again for 30 min at room temperature in the dark. DiSBAC₂(3) and VABSC remained in the wells during the assays.

Test compound concentrations are reported as the concentration seen by the cells at the beginning of the assay. No compounds were included in the add-back buffer, so the concentration dropped by a factor of two during the assay.

The optical filters were 400 \pm 8 nm for excitation, and 460 \pm 15 nm (donor) and 580 \pm 30 nm (acceptor) for emission. Unless otherwise specified, donor and acceptor emission intensities were recorded at 1 Hz. Background signals were obtained using multiwell plates containing the assay buffer only. Fluorescence emissions were recorded for 10 s to establish a baseline fluorescence ratio. Then, a volume of stimulus buffer equal to the volume already in the well (100 μ L for 96-well plates, 50 μ L for 384 well plates) was added.

Data analysis. Primary analysis was performed using VIPRData 2.0 from Aurora Discovery. The normalized fluorescence ratio $\Phi(t)$ is defined as the background-subtracted donor/acceptor ratios normalized to unity at the start of an assay:

$\Phi(t) = \left(\frac{D(t) - D_0}{A(t) - A_0} \right) \left(\frac{A(0) - A_0}{D(0) - D_0} \right),$	Equation 1
--	-------------------

where $D(t)$ and $A(t)$ are the donor and acceptor emission intensities at time t , and D_0 and A_0 are the background intensities. Changes in $\Phi(t)$ are linearly related to changes in the cell membrane potential V_m [54]. A positive change in membrane potential pulls oxonol away from the outer leaflet of the membrane, leading to an increase in donor signal and a decrease in acceptor signal. Therefore, positive $\Phi(t)$ indicates a depolarization of the membrane potential.

The 'screening window' z' [53] was used to describe the quality of the assay:

$z' = 1 - 3 \left(\frac{\delta N + \delta P}{ N - P } \right),$	Equation 2
--	-------------------

where $N \pm \delta N$ and $P \pm \delta P$ are the means and standard deviations of the responses of the negative and positive controls. This parameter has a theoretical maximum of one when there is no scatter in the control responses, and falls to zero when the difference between the control populations is three standard deviations. We require $z' > 0.5$ for quality control.

Linear and non-linear fitting were performed using Origin 7 (Originlab, Northampton, MA).

High throughput screen. Compounds were screened for antagonist activity at 10 μ M. Test compounds were stored at 400 mM in 30% DMSO/10 mM HEPES/water in 96-well plates. A 20:1 dilution into intermediate 96-well plates containing the 2X oxonol solution were performed using a RapidPlate (Caliper Life Sciences, Hopkinton, MA). The contents of four such intermediate plates were added to a 384-well plate containing HEK-HCN1 cells stained with CC2-DMPE for a further 2:1 dilution. Cell plates were prepared in groups of 6. For quality control, one column of each 384-well plate contained a serial dilution of ZD-7288, and another column contained 8 wells each of positive and negative controls (30 μ M ZD-7288). Acceptance criteria were $z' > 0.5$ for the control wells, and $6.4 < \text{pIC}_{50} < 7.2$ for the ZD-7288 dose-response. Data were normalized to the positive and negative controls on each plate.

Estimation of reversal potentials. The reversal potential for current through the HCN1 channel was estimated using the Goldman-Hodgkin-Katz (GHK) equation [55]:

$V_0 = \frac{RT \ln 10}{F} \log \left(\frac{P_{Na} [Na]_o + P_K [K]_o}{P_{Na} [Na]_i + P_K [K]_i} \right).$	Equation 3
--	-------------------

We assumed $RT \ln 10 / F = 59$ mV, $P_{Na} / P_K = 0.25$ [7], intracellular sodium $[Na]_i = 10$ mM, and intracellular potassium $[K]_i = 120$ mM.

Electrophysiology. Cells were plated on glass coverslips (12 mm round) in growth medium 24-48 h prior to testing. The intracellular solution contained (concentrations in mM): 120 KCl, 10 NaCl, 2 Mg-ATP, 0.5 CaCl₂, 2 MgCl₂, 10 HEPES, 5 EGTA free acid, 100 μ M cAMP, pH 7.4 with KOH, 290 mOs and was either made fresh or kept frozen until use to avoid degradation of ATP. Recording electrodes had resistances of 2-3 M Ω . The ground electrode was a chlorinated silver wire in intracellular solution, separated from

the cell bath with a 3M KCl agar bridge, to null the junction potentials. Antagonism was determined by serial additions of increasing concentrations of test compound, while measuring the current at a membrane potential of -100 mV.

ACKNOWLEDGEMENTS

The authors would like to thank Shaoming Huang for advice and technical expertise during the course of this work.

REFERENCES

- [1] Govrin-Lippmann, R.; Devor, M. *Brain Res.*, **1978**, *159*, 406-10.
- [2] Kajander, K.C.; Bennett, G.J. *J. Neurophysiol.*, **1992**, *68*, 34-44.
- [3] Brown, H.F.; DiFrancesco, D.; Noble, S.J. *Nature*, **1979**, *280*, 235-6.
- [4] Halliwell, J.V.; Adams, P.R. *Brain Res.*, **1982**, *250*, 71-92.
- [5] Santoro, B.; Grant, S.G.; Bartsch, D.; Kandel, E.R. *Proc. Natl. Acad. Sci. USA.*, **1997**, *94*, 14815-20.
- [6] Ludwig, A.; Zong, X.; Hofmann, F.; Biel, M. *Cell. Physiol. Biochem.*, **1999**, *9*, 179-86.
- [7] Ludwig, A.; Zong, X.; Jeglitsch, M.; Hofmann, F.; Biel, M. *Nature*, **1998**, *393*, 587-91.
- [8] Brown, S.M.; Dubin, A.E.; Chaplan, S.R. *Pain Pract.*, **2004**, *4*, 182-93.
- [9] Scroggs, R.S.; Todorovic, S.M.; Anderson, E.G.; Fox, A.P. *J. Neurophysiol.*, **1994**, *71*, 271-9.
- [10] Yagi, J.; Sumino R. *J. Neurophysiol.*, **1998**, *80*, 1094-104.
- [11] Cardenas, C.G.; Mar, L.P.; Vysokanov, A.V.; Arnold, P.B.; Cardenas, L.M.; Surmeier, D.J.; Scroggs, R.S. *J. Physiol.*, **1999**, *518*(Pt 2), 507-23.
- [12] Villiere, V.; McLachlan, E.M. *J. Neurophysiol.*, **1996**, *76*, 1924-41.
- [13] Abdulla, F.A.; Smith, P.A. *J. Neurophysiol.*, **2001**, *85*, 630-43.
- [14] Abdulla, F.A.; Smith, P.A. *J. Neurophysiol.*, **2001**, *85*, 644-58.
- [15] Yao, H.; Donnelly, D.F.; Ma, C.; LaMotte, R.H. *J. Neurosci.*, **2003**, *23*, 2069-74.
- [16] Chaplan, S.R.; Guo, H.Q.; Lee, D.H.; Luo, L.; Liu, C.; Kuei, C.; Velumian, A.A.; Butler, M.P.; Brown, S.M.; Dubin, A.E. *J. Neurosci.*, **2003**, *23*, 1169-78.
- [17] Tu, H.; Deng, L.; Sun, Q.; Yao, L.; Han, J.S.; Wan, Y. *J. Neurosci. Res.*, **2004**, *76*, p. 713-22.
- [18] Masuda, N.; Hayashi, Y.; Matsuyoshi, H.; Chancellor, M.B.; de Groat, W.C.; Yoshimura, N. *Brain Res.*, **2006**, *1096*, 40-52.
- [19] Mayer, M.L.; Westbrook, G.L. *J. Physiol.*, **1983**, *340*, 19-45.
- [20] Pearce, R.J.; Duchon, M.R. *Neuroscience*, **1994**, *63*, 1041-56.
- [21] Raes, A.; Van de Vijver, G.; Goethals, M.; van Bogaert, P.P. *Br. J. Pharmacol.*, **1998**, *125*, 741-50.
- [22] Stansfeld, C.E.; Wallis, D.I. *J. Neurophysiol.*, **1985**, *54*, 245-60.
- [23] Doan, T.N.; Kunze, D.L. *J. Physiol.*, **1999**, *514*(Pt 1), 125-38.
- [24] Linden, D.R.; Sharkey, K.A.; Mawe, G.M. *J. Physiol.*, **2003**, *547*(Pt 2), 589-601.
- [25] Villiere, V.; McLachlan, E.M. *J. Neurophysiol.*, **1996**, *76*, 1924-41.
- [26] Takigawa, T.; Alzheimer, C.; Quasthoff, S.; Grafe, P. *Neuroscience*, **1998**, *82*, 631-4.
- [27] Frishman, W.H.; Pepine, C.J.; Weiss, R.J.; Baiker, W.M. *J. Am. Coll. Cardiol.*, **1995**, *26*, 305-12.
- [28] Lee, D.H.; Chang, L.; Sorkin, L.S.; Chaplan, S.R. *J. Pain*, **2005**, *6*, 417-24.
- [29] Sun, Q.; Xing, G.G.; Tu, H.Y.; Han, J.S.; Wan, Y. *Brain Res.*, **2005**, *1032*, 63-9.
- [30] Dalle, C.; Eisenach, J.C. *Reg. Anesth. Pain Med.*, **2005**, *30*, 243-8.
- [31] Luo, L.; Chang, L.; Brown, S.M.; Ao, H.; Lee, D.H.; Higuera, E.S.; Dubin, A.E.; Chaplan, S.R. *Neuroscience*, **2007**, *144*, 1477-85.
- [32] Pape, H.C. *Annu. Rev. Physiol.*, **1996**, *58*, 299-327.
- [33] Czeh, G.; Kudo, N.; Kuno, M. *J. Physiol.*, **1977**, *270*, 165-80.
- [34] Gallego, R.; Ivorra, I.; Morales, A. *J. Physiol.*, **1987**, *391*, 39-56.
- [35] Wells, J.E.; Rowland, K.C.; Proctor, E.K. *Int. Endod. J.*, **2007**, *40*, 715-21.
- [36] Iwata, K.; Tsuboi, Y.; Shima, A.; Harada, T.; Ren, K.; Kanda, K.; Kitagawa, J. *J. Orofac. Pain*, **2004**, *18*, 293-8.
- [37] Ingram, S.L.; Williams, J.T. *J. Physiol.*, **1996**, *492*(Pt 1), 97-106.
- [38] Jafri, M.S.; Weinreich, D. *J. Neurophysiol.*, **1998**, *79*, 769-77.
- [39] Moosmang, S.; Stieber, J.; Zong, X.; Biel, M.; Hofmann, F.; Ludwig, A. *Eur. J. Biochem.*, **2001**, *268*, 1646-52.
- [40] Doan, T.N.; Stephans, K.; Ramirez, A.N.; Glazebrook, P.A.; Andresen, M.C.; Kunze, D.L. *J. Neurosci.*, **2004**, *24*, 3335-43.

- [41] Antal, M.; Papp, I.; Bahaerguli, N.; Veress, G.; Vereb, G. *Eur. J. Neurosci.*, **2004**, *19*, 1336-42.
- [42] Papp, I.; Szucs, P.; Holló, K.; Erdélyi, F.; Szabó, G.; Antal, M. *Eur. J. Neurosci.*, **2006**, *24*, 1341-52.
- [43] Matsuyoshi, H.; Masuda, N.; Chancellor, M.B.; Erickson, V.L.; Hirao, Y.; de Groat, W.C.; Wanaka, A.; Yoshimura, N. *Brain Res.*, **2006**, *1119*, 115-23.
- [44] Milligan, C.J., EdwardsLJ.; Deuchars, J. *Brain Res.*, **2006**, *1081*, 79-91.
- [45] Robinson, R.B.; Siegelbaum, S.A. *Annu. Rev. Physiol.*, **2003**, *65*, 453-80.
- [46] Ludwig, A.; Zong, X.; Stieber, J.; Hullin, R.; Hofmann, F.; Biel, M. *EMBO J.*, **1999**, *18*, 2323-9.
- [47] Stieber, J.; Stöckl, G.; Herrmann, S.; Hassfurth, B.; Hofmann, F. *J. Biol. Chem.*, **2005**, *280*, 34635-43.
- [48] Chen, S.; Wang, J.; Siegelbaum, S.A. *J. Gen. Physiol.*, **2001**, *117*, 491-504.
- [49] Raes, A.; Wang, Z.; van den Berg, R.J.; Goethals, M.; Van de Vijver, G.; van Bogaert, P.P. *Pflugers Arch.*, **1997**, *434*, 543-50.
- [50] Maher, M.P.; Wu, N.T.; Ao, H. *J. Biomol. Screen.*, **2007**, *12*, 656-667
- [51] Wood, C.; Williams, C.; Waldron, G.J. *Drug Discov. Today.*, **2004**, *9*, 434-41.
- [52] González, J.E.; Oades, K.; Leychikis, Y.; Harootunian, A.; Negulescu, P.A. *Drug Discov. Today*, **1999**, *4*, 431-439.
- [53] Zhang, J.H.; Chung, T.D.; Oldenburg, K.R. *J. Biomol. Screen.*, **1999**, *4*, 67-73.
- [54] González, J.E.; Tsien, R.Y. *Chem. Biol.*, **1997**, *4*, 269-77.
- [55] Hille, B. *Ionic Channels of Excitable Membranes*. Second ed.. Sunderland, Massachusetts: Sinauer Associates, **1992**.

Received: December 21, 2007

Revised: January 18, 2008

Accepted: January 18, 2008